THE JOURNAL OF PHYSICAL CHEMISTRY A

Article

pubs.acs.org/JPCA

Chalcogen Bonds in Complexes of SOXY (X, Y = F, Cl) with Nitrogen Bases

Luis Miguel Azofra,[†] Ibon Alkorta,[†] and Steve Scheiner*[,‡]

[†]Instituto de Química Médica, CSIC, Juan de la Cierva, 3, E-28006 Madrid, Spain

[‡]Department of Chemistry and Biochemistry, Utah State University, Logan, Utah 84322-0300, United States

Supporting Information

ABSTRACT: SOF_2, SOFCl, and $SOCl_2$ were each paired with a series of N bases. The potential energy surface of the binary complexes were characterized by MP2 calculations with double and triple-ξ basis sets, extrapolated to complete sets. The most stable configurations contained a S···N chalcogen bond with interaction energies as high as 6.8 kcal/mol. These structures are stabilized by a $N_{lp} \rightarrow \sigma^*(S-Z)$ electron transfer (Z = O, F, Cl), complemented by Coulombic attraction of N to the σ-hole opposite the Z atom. N···S−F and N···S−Cl chalcogen bonds are stronger than N···S═O interactions. Formation of each chalcogen bond elongates all of the internal covalent bonds within SOXY, especially the S−Cl bond. Halogen-bonded (N···Cl−S) complexes were also observed, but these are more weakly bound, by less than 3 kcal/mol.

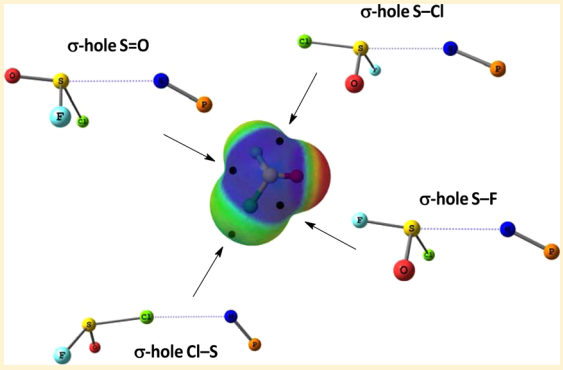

INTRODUCTION

The importance of noncovalent interactions[1] resides in the key role that they play as attractive forces which hold together a wide range of dimers and larger aggregates. In that sense, they are also essential ingredients in the structure adopted by many single molecules, as they can represent large fractions of the forces between segments that are not covalently bonded to one another. Hydrogen,[2−5] halogen,[6−11] pnicogen,[12−24] and tetrel[25−28] bonds are a few examples of noncovalent interactions, where the name signifies the identity of the bridging atom. Another member of this group is the chalcogen bond[29−40] which arises when a member of the chalcogen family (Y), e.g. O, S, Se, or Te, is drawn toward another electronegative atom (X). Coulombic attractions are supplemented by charge transfer from the lone pair(s) of the X atom into the σ^* or π^* antibonding Z−Y orbitals (where Z is covalently bonded to Y), which tends to weaken and lengthen the latter Z−Y bond.[41−44]

The molecular electrostatic potential (MEP) of each monomer can be characterized by the presence of maxima and minima, which represent plausible binding sites. A strong Coulombic attraction can be anticipated as the maximum in the MEP of one molecule approaches a minimum in its partner. Minima are typically associated with lone electron pair(s). Maxima can usually be classified into two main groups: (i) σ-holes, which are localized along the extension of the Z−Y bond; and (ii) π-holes, which are situated above the molecular plane.[42,45−47] In connection with the latter, computational efforts have also examined chalcogen bonds associated with π-holes in monomers such as O_3,[39,48] SO_2,[38,43,44] or SO_3.[40]

With respect to the σ-holes, most studies to date have dealt with molecules which contain only one or at most two such positive regions in the MEP. Molecules such as SOXY, where X and Y are both halogen atoms present an interesting scenario. This molecule ought to contain a σ-hole on the S-end of each S−X, S−Y, or S═O bond for a total of as many as 3 positive regions. Interaction through the S end would result in a chalcogen bond, while the participation of a positive hole on the other end would be associated with a halogen bond when X, Y = Cl. Study of this molecule can thus address a number of different questions. How do the chalcogen and halogen bonds compare in terms of not only strength, but also electronic properties? What is the effect of replacing one halogen, F, with another like Cl? How does the monomer respond when it forms a chalcogen bond on the S end of the S−X bond, vs a halogen bond on the other end? In order to address these questions, three different SOXY molecules were considered: SOF_2, SOFCl, and $SOCl_2$. Each of these molecules was allowed to interact with a series of N-bases of varying electron-donating capability: $NHCH_2$, NH_3, PN, HCN, and N_2.

COMPUTATIONAL DETAILS

The geometries of binary complexes between thionyl difluoride (SOF_2), thionyl fluoride chloride (SOFCl), and thionyl dichloride ($SOCl_2$) and the nitrogen bases methanimine ($NHCH_2$), ammonia (NH_3), phosphorus nitride (PN), hydrogen cyanide (HCN), and dinitrogen (N_2) were optimized by

Received: November 26, 2014
Revised: December 29, 2014
Published: December 29, 2014

Downloaded via UNIV LAS PALMAS GRAN CANARIA on October 28, 2020 at 09:31:53 (UTC).
See https://pubs.acs.org/sharingguidelines for options on how to legitimately share published articles.

© 2014 American Chemical Society

DOI: 10.1021/jp511828h
J. Phys. Chem. A 2015, 119, 535−541

means of the second-order Møller−Plesset perturbation theory (MP2)[49] using the aug-cc-pVDZ basis set.[50,51] Searches on the potential energy surface (PES) were carried out by using the ESP maxima and minima of each monomer as a guide, calculated via the WFA-SAS program.[52] In order to obtain more accurate structures, reoptimization at the MP2/aug-cc-pVTZ computational level was performed. All structures were verified as true minima by virtue of all positive vibrational frequencies. Calculations were carried out via the Gaussian 09 package (revision D.01).[53]

Interaction energies, E_{int}, were computed as the difference in energy between the complex on one hand, and the sum of the energies of the monomers on the other, with monomer geometries the same as in the complex. These interaction energies were corrected for basis set superposition error (BSSE) by the counterpoise procedure. E_{int} was also extrapolated to the limit of the complete basis set (CBS) using the Truhlar procedure that showed promise earlier in the consideration of other related complexes, and using the BSSE-corrected energies at double and triple-ξ.[54,55]

Atoms in molecules (AIM) theory[56,57] at MP2-level and natural bond orbital (NBO) theory[58] with the ωB97XD functional,[59] both with the aug-cc-pVTZ basis set, were applied to help analyze the interactions, using the AIMAll[60] and NBO6.0[61] programs. This functional was chosen so as to efficiently incorporate the effects of electron correlation into the NBO prescription, as it represents a long-range corrected hybrid density functional with damped atom−atom dispersion correction.

RESULTS

Monomers. The halogenated thionyl SOF_2, SOFCl, and $SOCl_2$ monomers are all pyramidal, and adopt C_s, C_1, and C_s symmetry, respectively. Their molecular electrostatic potentials (MEP) on the 0.001 au electron density isosurface are presented in Figure 1 where black dots indicate the position

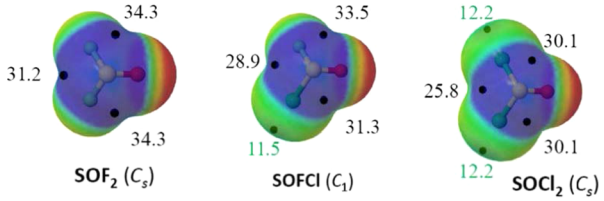

Figure 1. Molecular electrostatic potential (MEP) on the 0.001 au electron density isosurface for the pyramidal SOF_2, SOFCl, and $SOCl_2$ monomers, calculated at the MP2/aug-cc-pVTZ computational level. The red and blue colors correspond to negative and positive regions, respectively. Black dots indicate the location of the σ-hole MEP maxima on the surface, with numerical values displayed in kcal/mol; black numbers refer to incipient chalcogen bonds and green numbers to potential halogen bonds.

of these maxima, $V_{s,max}$, with numerical values displayed in kcal/mol. The intensity of the σ-hole opposite the S═O bond diminishes as F atoms are replaced by Cl. The S−X holes are a bit deeper with values exceeding 30 kcal/mol; the largest values are associated with the S−F bonds in SOF_2. In the case of S−Cl bonds, there is a much less intense σ-hole, with $V_{s,max}$ around 11−12 kcal/mol, along the extension of the S−Cl bond, at the Cl-end, which ought to facilitate formation of a halogen bond. There are minima in the potentials of the nitrogen bases, along the N lone pair direction, with $V_{s,min}$ equal to −37.2, −37.0, −31.9, −31.4, and −8.5 kcal/mol, respectively for NH_3, $NHCH_2$, HCN, PN, and N_2.

Heterodimers. Figure 2 displays samples of some of the structures obtained for the heterodimers comprising SOXY (X, Y = F, Cl) and nitrogen bases, specifically, those in which the lone pair of the nitrogen atom interacts with the σ-hole in sulfur. As indicated by the monomer potentials in Figure 1, the N atom can be situated opposite to the O or halogen atoms. The CH atoms in $NHCH_2$ present the possibility of a secondary CH···X H-bond, as for example in the SOFCl···$NHCH_2$ N···S−F complex, wherein R(H···Cl) = 2.846 Å. The presence of this H-bond is confirmed by NBO analysis which shows a $Cl_{lp} \rightarrow \sigma^*(CH)$ charge transfer $E^{(2)}$ of 0.60 kcal/mol, and also by AIM with ρ and $\nabla^2\rho$ values at the BCP of 0.008 and 0.029 au, respectively.

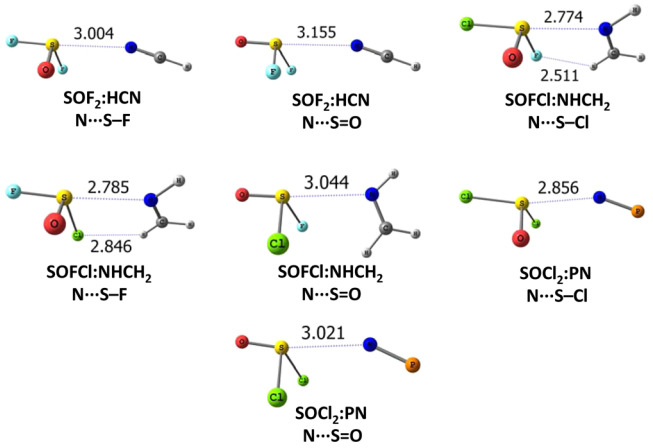

Figure 2. Structures of the SOXY:Z (X, Y = F, Cl and Z = HCN, $NHCH_2$, PN) complexes optimized at the MP2/aug-cc-pVTZ computational level supported by chalcogen bonds. Three kinds of dimers, attending to the presence of N···S═O or N···S−X (X = F, Cl) chalcogen bonds, can be discriminated. Blue dotted lines indicate noncovalent interactions corroborated via AIM with interatomic distances in Å.

All of the N···S chalcogen-bonded heterodimers are summarized in Table 1. Interaction energies are reported at both the aug-cc-pVDZ and aug-cc-pVTZ levels, using geometries optimized at their corresponding levels. Also shown are these same quantities extrapolated to the complete basis set limit. All interaction energies have been corrected for basis set superposition error by the counterpoise procedure. Interaction energies are converted to binding energies (E_b) in Table S1, which compare the energy of the complex with that of the monomers in their optimized geometries. E_b is thus related to E_{int} by the monomer strain energies. With respect to BSSE corrections, they become smaller as the basis set is enlarged. They amount to 46 and 22% corrections for the DZ and TZ cases, respectively.

There are several trends in Table 1 which are apparent upon inspection. In the first place, the interaction energies follow the pattern $NHCH_2$ > NH_3 > PN > HCN > N_2. Taking the N···S−Cl chalcogen bonds with $SOCl_2$ as an example, E_{int}^{CBS} is equal to −6.79, −6.03, −5.07, −3.93, and −1.62 kcal/mol in that order. This pattern is not restricted to the N···S−Cl chalcogen bond, but applies as well to N···S═O: −5.22, −4.37, −4.35, −3.38, and −1.54 kcal/mol. It may be noted that this ordering is somewhat different than the $V_{s,min}$ pattern: NH_3 > $NHCH_2$ > HCN > PN > N_2. In terms of the different sorts of chalcogen

DOI: 10.1021/jp511828h
J. Phys. Chem. A 2015, 119, 535−541

Table 1. Interaction Energy,[a] in kcal/mol, at the MP2/aug-cc-pVDZ, MP2/aug-cc-pVTZ and MP2/CBS Levels for the Chalcogen-Bonded Heterodimers Formed between SOXY (X, Y = F, Cl) and Nitrogen Bases[b]

acc.	donor	type	E_{int}^{DZ}	E_{int}^{TZ}	E_{int}^{CBS}	R(N···S)	$\rho_{N\cdots S}$	$\nabla^2\rho_{N\cdots S}$	$E^{(2)}{}_{N\cdots S}$
$NHCH_2$	$SOCl_2$	N···S−Cl	−6.74	−6.63	−6.79	2.753	0.0237	0.0677	9.88
$NHCH_2$	$SOCl_2$	N···S═O	−5.14	−5.16	−5.22	3.022	0.0142	0.0460	2.83
$NHCH_2$	SOFCl	N···S−Cl	−6.38	−6.14	−6.24	2.774	0.0224	0.0640	7.86
$NHCH_2$	SOFCl	N···S−F	−6.53	−6.31	−6.45	2.785	0.0217	0.0642	7.47
$NHCH_2$	SOFCl	N···S═O	−4.75	−4.67	−4.73	3.044	0.0132	0.0431	1.90
$NHCH_2$	SOF_2	N···S−F	−5.94	−5.54	−5.61	2.831	0.0195	0.0584	3.89
$NHCH_2$	SOF_2	N···S═O	−4.29	−4.08	−4.11	3.092	0.0116	0.0385	1.10
NH_3	$SOCl_2$	N···S−Cl	−6.08	−5.91	−6.03	2.779	0.0228	0.0637	11.09
NH_3	$SOCl_2$	N···S═O	−4.60	−4.43	−4.37	3.035	0.0139	0.0446	3.32
NH_3	SOFCl	N···S−Cl	−5.67	−5.50	−5.62	2.813	0.0209	0.0591	8.75
NH_3	SOFCl	N···S−F	−5.91	−5.63	−5.72	2.809	0.0209	0.0606	8.25
NH_3	SOFCl	N···S═O	−4.25	−4.03	−4.00	3.075	0.0125	0.0405	2.17
NH_3	SOF_2	N···S−F	−5.34	−5.02	−5.12	2.860	0.0185	0.0547	4.31
NH_3	SOF_2	N···S═O	−3.76	−3.47	−3.42	3.121	0.0110	0.0363	1.29
PN	$SOCl_2$	N···S−Cl	−4.80	−4.91	−5.07	2.856	0.0171	0.0572	3.71
PN	$SOCl_2$	N···S═O	−4.10	−4.23	−4.35	3.021	0.0127	0.0452	1.66
PN	SOFCl	N···S−Cl	−4.35	−4.41	−4.53	2.887	0.0158	0.0530	2.08
PN	SOFCl	N···S−F	−4.53	−4.57	−4.71	2.885	0.0158	0.0540	2.85
PN	SOFCl	N···S═O	−3.60	−3.67	−3.75	3.064	0.0114	0.0408	1.00
PN	SOF_2	N···S−F	−3.99	−3.95	−4.05	2.932	0.0141	0.0485	0.84
PN	SOF_2	N···S═O	−3.07	−3.06	−3.08	3.118	0.0100	0.0359	0.51
HCN	$SOCl_2$	N···S−Cl	−3.90	−3.87	−3.93	2.952	0.0136	0.0495	2.91
HCN	$SOCl_2$	N···S═O	−3.31	−3.36	−3.38	3.079	0.0110	0.0415	1.52
HCN	SOFCl	N···S−Cl	−3.68	−3.62	−3.66	2.975	0.0128	0.0465	2.03
HCN	SOFCl	N···S−F	−3.78	−3.69	−3.76	2.968	0.0129	0.0476	2.31
HCN	SOFCl	N···S═O	−3.02	−3.04	−3.09	3.114	0.0100	0.0379	0.93
HCN	SOF_2	N···S−F	−3.48	−3.33	−3.37	3.004	0.0118	0.0436	0.72
HCN	SOF_2	N···S═O	−2.69	−2.66	−2.69	3.155	0.0090	0.0343	0.51
N_2	$SOCl_2$	N···S−Cl	−1.35	−1.54	−1.62	3.177	0.0078	0.0317	1.01
N_2	$SOCl_2$	N···S═O	−1.29	−1.49	−1.54	3.268	0.0069	0.0281	0.64
N_2	SOFCl	N···S−Cl	−1.15	−1.30	−1.35	3.209	0.0072	0.0291	0.68
N_2	SOFCl	N···S−F	−1.26	−1.43	−1.51	3.196	0.0074	0.0301	0.82
N_2	SOFCl	N···S═O	−1.10	−1.24	−1.28	3.308	0.0061	0.0252	0.64
N_2	SOF_2	N···S−F	−1.07	−1.18	−1.23	3.235	0.0067	0.0272	0.24
N_2	SOF_2	N···S═O	−0.90	−0.99	−1.00	3.354	0.0054	0.0226	0.21

[a]Interaction energies corrected for BSSE via counterpoise procedure. [b]Also shown are intermolecular distance (Å), electron density and its Laplacian at the BCP (au), and second-order perturbation NBO energy, (kcal/mol) for $N_{lp} \rightarrow \sigma^*$[S(X/Y)] transfers.

bond, N···S−X > N···S═O which conforms to the idea that the σ-holes are a bit deeper opposite the halogen than the O atoms in Figure 1. In the case of the SOFCl molecule, there is a slight preference for S−F over S−Cl, which is contrary to the σ-hole depth. Another discrepancy emerges in the comparison of the three SOXY molecules: $SOCl_2$ forms the strongest complexes even though it has the weakest S−X σ-holes. These discrepancies highlight the fact that these interactions are not governed solely by electrostatic forces.

Also displayed in Table 1 are the intermolecular N···S distances in the optimized heterodimers. These distances fit the expected pattern of shorter distances being associated with stronger complexes. In fact, there is a strong correlation between these two quantities as visible in Figure 3a, whether one is examining N···S═O or N···S−X chalcogen bonds. AIM analysis of these chalcogen bonds provides additional data, chief among them the electron density ρ, and its Laplacian $\nabla^2\rho$, at the BCP. These quantities are listed in Table 1, and their smooth correlation with the interaction energy, illustrated in Figure 3b,c, respectively. The last column of Table 1 contains the NBO charge transfer energy $E^{(2)}$ which corresponds to the $N_{lp} \rightarrow \sigma^*$(S−Y) transfer. As anticipated, large transfer energies correspond to stronger interactions, as observed in Figure 3d.

It is interesting to examine the relationships between E_{int} and the geometric R(N···S), electronic (ρ and $\nabla^2\rho$), and NBO $E^{(2)}$ properties of these chalcogen bonds. As can be seen in Figure 3a, E_{int} at the MP2/CBS level has an exponential relationship with the R(N···S) interatomic distance; N···S−X and N···S═O bonds have correlation coefficients of 0.99 and 0.93, respectively. The relationship of E_{int} to ρ is also an exponential one, with R^2 = 0.99 and 0.96 for N···S−X and N···S═O, respectively. In contrast, $\nabla^2\rho$, is linearly related to E_{int} with corresponding correlation coefficients of 0.99 and 0.93. Correlations are poorer for $E^{(2)}$, as is evident in Figure 3d, although there is a clear pattern of larger values of $E^{(2)}$ as the interaction energy climbs.[34,38]

As has been indicated previously, the formation of a chalcogen bond typically places additional electron density into the σ^* antibonding orbital which lies directly opposite the N lone pair. This transfer can be expected to elongate the relevant bond S−Z bond length. Such a trend was observed here as well, but there are certain interesting refinements that

DOI: 10.1021/jp511828h
J. Phys. Chem. A 2015, 119, 535−541

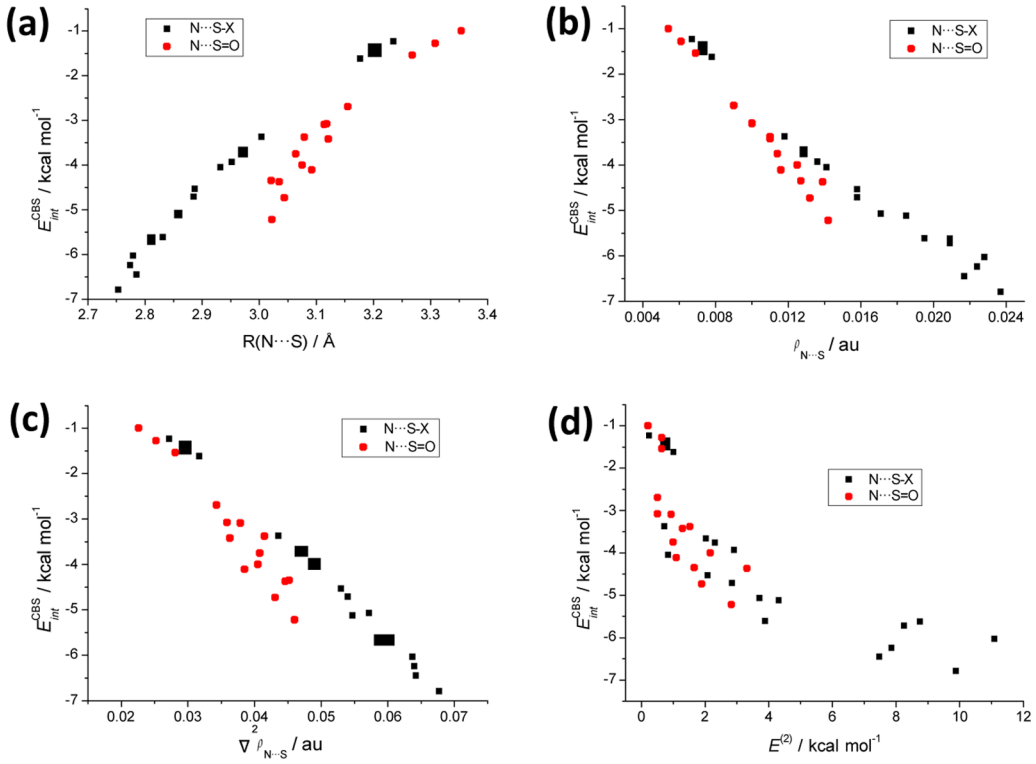

Figure 3. E_{int} at MP2/CBS level vs: (a) interatomic R(N···S) distance, in Å; (b) $\rho_{N\cdots S}$ at the BCP, in au; (c) $\nabla^2\rho_{N\cdots S}$ at the BCP, in au; and (d) $E^{(2)}_{N\cdots S}$, in kcal/mol, for the chalcogen bonds in Table 1.

were observed along with this gross pattern. For example, formation of the N···S═O configurations elongates R(S═O) but by a relatively small amount, less than 3 mÅ in all cases. (All bond length changes resulting from the formation of the N···S═O chalcogen bond are displayed in the Supporting Information (SI), Table S2.) When these noncovalent bonds are formed, the R(S−X) bonds involving the peripheral halogen atoms are stretched by a good deal more. R(S−F) elongates by as much as 6 mÅ. But it is the R(S−Cl) bond that stretches the most, by as much as 22 mÅ. Formation of the N···S−F chalcogen bond has little effect upon R(S═O), but R(S−F) stretches by up to 16 mÅ, and R(S−Cl) by up to 27 mÅ, as may be seen in SI, Table S3. The largest perturbations arise in the N···S−Cl geometries which are reported in Table 2. The S−Cl bond elongates by as much as 33 mÅ. In summary, there is a general correlation between bond stretches and the strength of the chalcogen bond. But as a general rule, the S−Cl bond undergoes the largest stretch, followed by R(S−F) and then R(S═O). Each of these stretches is magnified when it is the pertinent σ^* antibonding orbital which is the recipient of the charge being transferred from the N lone pair, but this pattern remains in force regardless of the particular Z atom in the N···S−Z chalcogen bond. S−Cl bond elongations in complexes containing the N···S−Cl motif reflect a linear correlation between their magnitudes and the ρ and $\nabla^2\rho$ values at the BCP with R^2 = 0.87 and 0.89, respectively. The correlation is considerably poorer between Δr(S−Cl) and the NBO charge transfer energy.

Table 2. Changes in Bond Lengths (mÅ) Caused by Formation of N···S−Cl Bonds

acceptor	donor	ΔR(S═O)	ΔR(S−Cl)	ΔR(S−X[a])
$NHCH_2$	$SOCl_2$	−1.3	28.9	22.1[b]
$NHCH_2$	SOFCl	−0.4	33.1	8.3[c]
NH_3	$SOCl_2$	−0.4	25.1	20.9[b]
NH_3	SOFCl	1.1	28.3	3.9[c]
PN	$SOCl_2$	−0.5	18.6	10.4[b]
PN	SOFCl	0.3	22.4	0.0[c]
HCN	$SOCl_2$	−0.8	16.6	7.1[b]
HCN	SOFCl	−0.2	20.5	−1.0[c]
N_2	$SOCl_2$	0.0	2.0	3.4[b]
N_2	SOFCl	0.4	3.4	0.4[c]

[a]X = halogen not involved in N···S−Cl bond, either Cl or F. [b]X = Cl. [c]X = F.

As the S−Cl bonds experience the largest stretch upon complexation, the S−Cl stretching vibrational frequencies in the most stable complexes $SOCl_2$:Z and SOFCl:Z (Z = $NHCH_2$, NH_3) are gathered in SI, Table S5. These frequencies are shifted to the red by −20.5 and −17.4 cm^{-1} for the symmetric mode in the $SOCl_2$:$NHCH_2$ and $SOCl_2$:NH_3 N···S−Cl complexes, respectively, and −12.4 and −3.6 cm^{-1} for the antisymmetric mode. In those cases in which the chalcogen bond donor is the SOFCl species, the largest red shift occurs when the chalcogen bond acceptor interacts with SOFCl via the σ-hole associated with the aforementioned S−Cl, with values of −22.7 and −17.1 cm^{-1} in which Z is $NHCH_2$ and NH_3 and the smaller amounts of −12.7 and −8.2 cm^{-1} for the N···S−F type.

Figure 1 showed that there are also σ-holes along the extension of the S−Cl bonds in SOFCl and $SOCl_2$. These holes are considerably smaller than those on the S side, but nonetheless offer a positive region of the MEP with which a N-base can interact. Indeed, halogen-bonded complexes present local minima in the potential energy surface of these two molecules with the N-bases. Examples of two such structures are illustrated in Figure 4. The energies and

DOI: 10.1021/jp511828h
J. Phys. Chem. A 2015, 119, 535−541

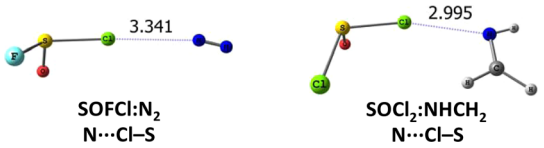

Figure 4. Structures of the $SOFCl{:}N_2$ and $SOCl_2{:}NHCH_2$ complexes optimized at the MP2/aug-cc-pVTZ computational level supported by halogen bonds. Blue dotted lines indicate noncovalent interactions corroborated via AIM with interatomic distances in Å.

intermolecular distance of all of these minima are reported in Table 3, where interaction energies vary between −0.64 and

Table 3. Interaction Energy[a] (kcal/mol) and Intermolecular Distance (Å), at the MP2/aug-cc-pVTZ level for the Halogen-Bonded Heterodimers of SOXCl (X = F, Cl)

acc.	donor	type	E_{int}^{TZ}	R(N···Cl)
$NHCH_2$	$SOCl_2$	N···Cl–S	−2.56	2.995
$NHCH_2$	SOFCl	N···Cl–S	−2.31	3.039
NH_3	$SOCl_2$	N···Cl–S	−1.95	3.084
NH_3	SOFCl	N···Cl–S	−1.71	3.145
PN	$SOCl_2$	N···Cl–S	−2.06	3.012
PN	SOFCl	N···Cl–S	−1.85	3.055
HCN	$SOCl_2$	N···Cl–S	−1.54	3.129
HCN	SOFCl	N···Cl–S	−1.40	3.166
N_2	$SOCl_2$	N···Cl–S	−0.69	3.308
N_2	SOFCl	N···Cl–S	−0.64	3.341

[a]Interaction energies corrected for BSSE via counterpoise procedure.

−2.56 kcal/mol. As expected by the smallness of the σ-holes, these heterodimers are considerably weaker than chalcogen-bonded structures in Table 1. Nonetheless, the same pattern of bonding energy is observed: $NHCH_2$ > NH_3 > PN > HCN > N_2. And again $SOCl_2$ is a slightly better Lewis acid than SOFCl. The binding energies of these same complexes are displayed along with the interaction energies in SI, Table S4, and obey the same trends.

The formation of each complex involves a redistribution of electron density. These density shifts are pictured in Figure 5 as the density of the complex minus the sum of the densities of the individual monomers. The systems chosen pair SOFCl with NH_3, in all four of the different configurations adopted by this

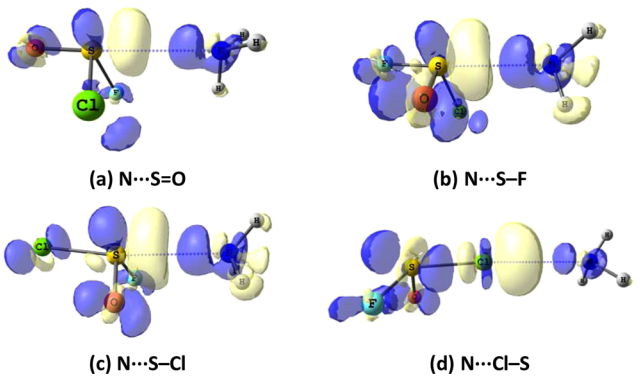

Figure 5. Electron density shifts occurring in (a) N···S═O; (b) N···S–F; (c) N···S–Cl chalcogen-bonded; and (d) N···Cl–S halogen-bonded complexes of SOFCl with NH_3. Blue/yellow regions represent gain/loss of density. Isocontours shown are ±0.001 au in (a–c) and ±0.0005 au in (d).

pair. The chalcogen-bonded complexes in Figure 5a–c are all similar in that a (blue) buildup of density occurs in the N lone pair region, and a yellow loss directly to the right of the S atom. Gains are noted also around all three of the S substituents, O, F, and Cl. The latter is consistent with the elongations of the various S═O and S–X bonds. The N···Cl–S halogen-bonded heterodimer in Figure 5d conforms to the expected pattern for such bonds. The most prominent feature is the density loss to the right of the Cl atom, with gains noted in other regions of the SOFCl molecule.

The molecular electrostatic potentials displayed in Figure 1 show that the positive region surrounding the central S atom does not have a maximum directly above S. It is thus not surprising to find there were no minima in the potential energy surface of any of these SOXY molecules in which the N base approaches S from above. In a similar vein, searches for possible minima associated with N···F–S halogen-bonded complexes all failed, consistent with the absence of a σ-hole associated with the F atom in the SOF_2 and SOFCl species.

CONCLUSIONS

Nitrogen bases of varying strengths, ranging from N_2 up to $NHCH_2$, all engage in S···N chalcogen bonds with SOF_2, SOFCl, and $SOCl_2$. The latter molecule forms the strongest bonds, followed by SOFCl and then SOF_2. With regard to the bases, bond strength follows the trend: $NHCH_2$ > NH_3 > PN > HCN > N_2. The N atom lines up opposite one of the three atoms that surround the S such that charge is transferred from the N lone pair to the corresponding σ^*(S–Z) antibonding orbital. N···S–X bonds are stronger than N···S═O, but there is no clear rule differentiating N···S–F from N···S–Cl, which are generally rather similar. There is a Coulombic component wherein the negative potential of the N-base aligns with a σ-hole opposite the Z–S bond, but the bond strengths do not correlate quantitatively with the depth of this σ-hole. Better correlations are observed between the bond strength and the electron density, and its Laplacian, at the AIM bond critical points. Formation of any of these chalcogen bonds elongates all of the covalent bonds within SOXY. The S–Cl bond stretch is most sensitive to chalcogen bond formation, followed by S–F and the S═O. Each stretch is magnified when the bond in question lies directly opposite the approaching N atom. The presence of a σ-hole along the extension of each S–Cl bond (but not S–F) permits formation of halogen bonds of the N···Cl–S type, but these bonds are considerably weaker than the chalcogen bonds.

In order to place the interactions described here in context, there are few complexes which incorporate a σ-hole around polyvalent S into a chalcogen bond. S···O chalcogen bonds involving SO_2 and a carbonyl, for example, are of the π-type, with interaction energies of some 6–7 kcal/mol.[38,43] The binding is somewhat weaker for SO_2 with N≡C nitriles, between 3 and 4 kcal/mol.[62] In the case of SO_3, these π S···O chalcogen bonds are somewhat stronger, rising up near 11 kcal/mol,[40] but are much weaker, on the order of 2 kcal/mol, if the partner molecule is as nonpolar as CO.[63] With respect to other trivalent S molecules $SO(CH_3)_2$ engages in a complex with CO_2 that contains a S···O chalcogen bond, with interaction energy of 2.6 kcal/mol.[64] Turning to tetravalent S, SF_4 can engage in a S···N chalcogen bond[7] with an amine, enlisting one of its σ-holes. The binding here is quite strong, as high as 14 kcal/mol, making SF_4 a more potent electron acceptor than SOXY.[65]

DOI: 10.1021/jp511828h
J. Phys. Chem. A 2015, 119, 535–541

■ ASSOCIATED CONTENT

Supporting Information

Binding and interaction energies in chalcogen-bonded complexes, changes in bond lengths for the N···S═O and N···S−F complexes, binding and interaction energies in halogen-bonded complexes, and S−Cl vibrational frequency changes. This material is available free of charge via the Internet at http://pubs.acs.org.

■ AUTHOR INFORMATION

Corresponding Author

*Fax: (+1) 435 797 3390. E-mail: steve.scheiner@usu.edu.

Notes

The authors declare no competing financial interest.

■ ACKNOWLEDGMENTS

This work has been supported by the CTQ2012-35513-C02-02 (MINECO) and S2013/MIT-2841 (Fotocarbon, Comunidad Autónoma de Madrid) Projects. Computer, storage, and other resources from the CTI (CSIC) and from the Division of Research Computing in the Office of Research and Graduate Studies at Utah State University are gratefully acknowledged.

■ REFERENCES

(1) Hobza, P.; Müller-Dethlefs, K. *Non-Covalent Interactions*; The Royal Society of Chemistry: Cambridge, U.K., 2009.

(2) Schuster, P.; Zundel, G.; Sandorfy, C. *The Hydrogen Bond. Recent Developments in Theory and Experiments*; North-Holland Publishing Co.: Amsterdam, The Netherlands, 1976.

(3) Scheiner, S. *Hydrogen Bonding: A Theoretical Perspective*; Oxford University Press: New York, USA, 1997.

(4) Grabowski, S. J. *Hydrogen Bonding - New Insights*; Springer: Dordrecht, The Netherlands, 2006.

(5) Gilli, G.; Gilli, P. *The Nature of the Hydrogen Bond*; Oxford University Press: Oxford, UK, 2009.

(6) Lommerse, J. P. M.; Stone, A. J.; Taylor, R.; Allen, F. H. The Nature and Geometry of Intermolecular Interactions between Halogens and Oxygen or Nitrogen. *J. Am. Chem. Soc.* **1996**, *118*, 3108−3116.

(7) Metrangolo, P.; Resnati, G. Halogen Versus Hydrogen. *Science* **2008**, *321*, 918−919.

(8) Zierkiewicz, W.; Michalska, D.; Zeegers-Huyskens, T. Theoretical Investigation of the Conformation, Acidity, Basicity and Hydrogen Bonding Ability of Halogenated Ethers. *Phys. Chem. Chem. Phys.* **2010**, *12*, 13681−13691.

(9) Adhikari, U.; Scheiner, S. Sensitivity of Pnicogen, Chalcogen, Halogen and H-Bonds to Angular Distortions. *Chem. Phys. Lett.* **2012**, *532*, 31−35.

(10) Politzer, P.; Murray, J. S.; Clark, T. Halogen Bonding and other σ-Hole Interactions: A Perspective. *Phys. Chem. Chem. Phys.* **2013**, *15*, 11178−11189.

(11) Solimannejad, M.; Malekani, M.; Alkorta, I. Substituent Effects on the Cooperativity of Halogen Bonding. *J. Phys. Chem. A* **2013**, *117*, 5551−5557.

(12) Del Bene, J. E.; Alkorta, I.; Sanchez-Sanz, G.; Elguero, J. $^{31}P-^{31}P$ Spin−Spin Coupling Constants for Pnicogen Homodimers. *Chem. Phys. Lett.* **2011**, *512*, 184−187.

(13) Scheiner, S. A New Noncovalent Force: Comparison of P···N Interaction with Hydrogen and Halogen Bonds. *J. Chem. Phys.* **2011**, *134*, 094315.

(14) Zahn, S.; Frank, R.; Hey-Hawkins, E.; Kirchner, B. Pnicogen Bonds: A New Molecular Linker? *Chem.—Eur. J.* **2011**, *17*, 6034−6038.

(15) Alkorta, I.; Sánchez-Sanz, G.; Elguero, J.; Del Bene, J. E. Influence of Hydrogen Bonds on the P···P Pnicogen Bond. *J. Chem. Theory Comput.* **2012**, *8*, 2320−2327.

(16) Alkorta, I.; Sánchez-Sanz, G.; Elguero, J.; Del Bene, J. E. Exploring $(NH_2F)_2$, $H_2FP{:}NFH_2$, and $(PH_2F)_2$ Potential Surfaces: Hydrogen Bonds or Pnicogen Bonds? *J. Phys. Chem. A* **2012**, *117*, 183−191.

(17) Scheiner, S. The Pnicogen Bond: Its Relation to Hydrogen, Halogen, and Other Noncovalent Bonds. *Acc. Chem. Res.* **2012**, *46*, 280−288.

(18) Alkorta, I.; Elguero, J.; Del Bene, J. E. Pnicogen Bonded Complexes of PO_2X (X = F, Cl) with Nitrogen Bases. *J. Phys. Chem. A* **2013**, *117*, 10497−10503.

(19) Alkorta, I.; Elguero, J.; Del Bene, J. E. Pnicogen-Bonded Cyclic Trimers $(PH_2X)_3$ with X = F, Cl, OH, NC, CN, CH_3, H, and BH_2. *J. Phys. Chem. A* **2013**, *117*, 4981−4987.

(20) Sánchez-Sanz, G.; Alkorta, I.; Trujillo, C.; Elguero, J. Intramolecular Pnicogen Interactions in $PHF-(CH_2)_n-PHF$ (n=2−6) Systems. *ChemPhysChem* **2013**, *14*, 1656−1665.

(21) Scheiner, S. Sensitivity of Noncovalent Bonds to Intermolecular Separation: Hydrogen, Halogen, Chalcogen, and Pnicogen Bonds. *CrystEngComm* **2013**, *15*, 3119−3124.

(22) Azofra, L. M.; Alkorta, I.; Elguero, J. Chiral Discrimination in Dimers of Diphosphines PH_2-PH_2 and PH_2-PHF. *ChemPhysChem* **2014**, *15*, 3663−3670.

(23) Bauzá, A.; Ramis, R.; Frontera, A. A Combined Theoretical and Cambridge Structural Database Study of π-Hole Pnicogen Bonding Complexes between Electron Rich Molecules and Both Nitro Compounds and Inorganic Bromides (YO_2Br, Y = N, P, and As). *J. Phys. Chem. A* **2014**, *118*, 2827−2834.

(24) Del Bene, J. E.; Alkorta, I.; Elguero, J. Pnicogen-Bonded Complexes $H_nF_{5-n}P{:}N$-Base, for n = 0−5. *J. Phys. Chem. A* **2014**, *118*, 10144−10154.

(25) Alkorta, I.; Rozas, I.; Elguero, J. Molecular Complexes between Silicon Derivatives and Electron-Rich Groups. *J. Phys. Chem. A* **2001**, *105*, 743−749.

(26) Azofra, L. M.; Altarsha, M.; Ruiz-López, M. F.; Ingrosso, F. A Theoretical Investigation of the CO_2-Philicity of Amides and Carbamides. *Theor. Chem. Acc.* **2013**, *132*, 1326.

(27) Bauzá, A.; Mooibroek, T. J.; Frontera, A. Tetrel-Bonding Interaction: Rediscovered Supramolecular Force? *Angew. Chem., Int. Ed.* **2013**, *52*, 12317−12321.

(28) Grabowski, S. J. Tetrel Bond-σ-Hole Bond as a Preliminary Stage of the S_N2 Reaction. *Phys. Chem. Chem. Phys.* **2014**, *16*, 1824−1834.

(29) Rosenfield, R. E.; Parthasarathy, R.; Dunitz, J. D. Directional Preferences of Nonbonded Atomic Contacts with Divalent Sulfur. 1. Electrophiles and Nucleophiles. *J. Am. Chem. Soc.* **1977**, *99*, 4860−4862.

(30) Burling, F. T.; Goldstein, B. M. Computational Studies of Nonbonded Sulfur-Oxygen and Selenium-Oxygen Interactions in the Thiazole and Selenazole Nucleosides. *J. Am. Chem. Soc.* **1992**, *114*, 2313−2320.

(31) Iwaoka, M.; Takemoto, S.; Tomoda, S. Statistical and Theoretical Investigations on the Directionality of Nonbonded S···O Interactions. Implications for Molecular Design and Protein Engineering. *J. Am. Chem. Soc.* **2002**, *124*, 10613−10620.

(32) Werz, D. B.; Gleiter, R.; Rominger, F. Nanotube Formation Favored by Chalcogen−Chalcogen Interactions. *J. Am. Chem. Soc.* **2002**, *124*, 10638−10639.

(33) Bleiholder, C.; Werz, D. B.; Köppel, H.; Gleiter, R. Theoretical Investigations on Chalcogen−Chalcogen Interactions: What Makes These Nonbonded Interactions Bonding? *J. Am. Chem. Soc.* **2006**, *128*, 2666−2674.

(34) Sánchez-Sanz, G.; Alkorta, I.; Elguero, J. Theoretical Study of the HXYH Dimers (X, Y = O, S, Se). Hydrogen Bonding and Chalcogen−Chalcogen Interactions. *Mol. Phys.* **2011**, *109*, 2543−2552.

(35) Jabłoński, M. Energetic and Geometrical Evidence of Nonbonding Character of Some Intramolecular Halogen···Oxygen and Other Y···Y Interactions. *J. Phys. Chem. A* **2012**, *116*, 3753−3764.

DOI: 10.1021/jp511828h
J. Phys. Chem. A 2015, 119, 535−541

(36) Sánchez-Sanz, G.; Trujillo, C.; Alkorta, I.; Elguero, J. Intermolecular Weak Interactions in HTeXH Dimers (X=O, S, Se, Te): Hydrogen Bonds, Chalcogen−Chalcogen Contacts and Chiral Discrimination. *ChemPhysChem* **2012**, *13*, 496−503.
(37) Adhikari, U.; Scheiner, S. Effects of Charge and Substituent on the S···N Chalcogen Bond. *J. Phys. Chem. A* **2014**, *118*, 3183−3192.
(38) Azofra, L. M.; Scheiner, S. Substituent Effects in the Noncovalent Bonding of SO_2 to Molecules Containing a Carbonyl Group. The Dominating Role of the Chalcogen Bond. *J. Phys. Chem. A* **2014**, *118*, 3835−3845.
(39) Azofra, L. M.; Alkorta, I.; Scheiner, S. An Exploration of the Ozone Dimer Potential Energy Surface. *J. Chem. Phys.* **2014**, *140*, 244311.
(40) Azofra, L. M.; Alkorta, I.; Scheiner, S. Strongly Bound Noncovalent $(SO_3)_n$:H_2CO complexes (n = 1, 2). *Phys. Chem. Chem. Phys.* **2014**, *16*, 18974−18981.
(41) Goettel, J. T.; Chaudhary, P.; Hazendonk, P.; Mercier, H. P. A.; Gerken, M. SF_4·$N(C_2H_5)_3$: The First Conclusively Characterized SF_4 Adduct with an Organic Base. *Chem. Commun.* **2012**, *48*, 9120−9122.
(42) Murray, J.; Lane, P.; Clark, T.; Riley, K.; Politzer, P. σ-Holes, π-Holes and Electrostatically-driven Interactions. *J. Mol. Model.* **2012**, *18*, 541−548.
(43) Azofra, L. M.; Scheiner, S. Complexation of n SO_2 Molecules (n = 1, 2, 3) with Formaldehyde and Thioformaldehyde. *J. Chem. Phys.* **2014**, *140*, 034302.
(44) Azofra, L. M.; Scheiner, S. Complexes Containing CO_2 and SO_2. Mixed Dimers, Trimers and Tetramers. *Phys. Chem. Chem. Phys.* **2014**, *16*, 5142−5149.
(45) Murray, J. S.; Lane, P.; Politzer, P. A Predicted New Type of Directional Noncovalent Interaction. *Int. J. Quantum Chem.* **2007**, *107*, 2286−2292.
(46) Politzer, P.; Murray, J.; Concha, M. σ-Hole Bonding between Like Atoms; A Fallacy of Atomic Charges. *J. Mol. Model.* **2008**, *14*, 659−665.
(47) Murray, J.; Lane, P.; Politzer, P. Expansion of the σ-Hole Concept. *J. Mol. Model.* **2009**, *15*, 723−729.
(48) Gadzhiev, O. B.; Ignatov, S. K.; Kulikov, M. Y.; Feigin, A. M.; Razuvaev, A. G.; Sennikov, P. G.; Schrems, O. Structure, Energy, and Vibrational Frequencies of Oxygen Allotropes O_n ($n \leq 6$) in the Covalently Bound and van der Waals Forms: *Ab Initio* Study at the CCSD(T) Level. *J. Chem. Theory Comput.* **2012**, *9*, 247−262.
(49) Møller, C.; Plesset, M. S. Note on an Approximation Treatment for Many-Electron Systems. *Phys. Rev.* **1934**, *46*, 618−622.
(50) Dunning, T. H. Gaussian Basis Sets for the Atoms Gallium through Krypton. *J. Chem. Phys.* **1977**, *66*, 1382−1383.
(51) Dunning, T. H. J. Gaussian Basis Sets for Use in Correlated Molecular Calculations. I. The Atoms Boron Through Neon and Hydrogen. *J. Chem. Phys.* **1989**, *90*, 1007−1023.
(52) Bulat, F.; Toro-Labbé, A.; Brinck, T.; Murray, J.; Politzer, P. Quantitative Analysis of Molecular Surfaces: Areas, Volumes, Electrostatic Potentials and Average Local Ionization Energies. *J. Mol. Model.* **2010**, *16*, 1679−1691.
(53) Frisch, M. J.; et al. *Gaussian 09*; Gaussian, Inc.: Wallingford, CT, 2009.
(54) Truhlar, D. G. Basis-set Extrapolation. *Chem. Phys. Lett.* **1998**, *294*, 45−48.
(55) Scheiner, S. Extrapolation to the Complete Basis Set Limit for Binding Energies of Noncovalent Interactions. *Comp. Theor. Chem.* **2012**, *998*, 9−13.
(56) Bader, R. F. W. *Atoms in Molecules: A Quantum Theory*; Clarendon Press: Oxford, U.K., 1990.
(57) Popelier, P. L. A. *Atoms In Molecules. An introduction*; Prentice Hall: Harlow, U.K., 2000.
(58) Weinhold, F. and Landis, C. R. *Valency and Bonding. A Natural Bond Orbital Donor-Aceptor Perspective*; Cambridge Press: Cambridge, U.K., 2005.
(59) Chai, J.-D.; Head-Gordon, M. Long-range Corrected Hybrid Density Functionals with Damped Atom-Atom Dispersion Corrections. *Phys. Chem. Chem. Phys.* **2008**, *10*, 6615−6620.
(60) Keith, T. A., TK Gristmill Software, Overland Park KS, USA, 2013.
(61) Glendening, E. D., Badenhoop, J. K., Reed, A. E., Carpenter, J. E., Bohmann, J. A., Morales, C. M., Landis, C. R. and Weinhold, F. *Theoretical Chemistry Institute*; University of Wisconsin: Madison, WI, 2013.
(62) Esrafili, M. D.; Vakili, M.; Solimannejad, M. Cooperative Interaction between π-Hole and Single-electron σ-Hole Interactions in O_2S···NCX···CH_3 and O_2Se···NCX···CH_3 Complexes (X = F, Cl, Br and I). *Mol. Phys.* **2014**, *112*, 2078−2084.
(63) Azofra, L. M.; Alkorta, I.; Scheiner, S. Noncovalent Interactions in Dimers and Trimers of SO_3 and CO. *Theor. Chem. Acc.* **2014**, *133*, 1586.
(64) Phuong, V. T.; Trang, N. T. T.; Vo, V.; Trung, N. T. A Comparative Study on Interaction Capacity of CO_2 with the >S═O and >S═S Groups in Some Doubly Methylated and Halogenated Derivatives of CH_3SOCH_3 and CH_3SSCH_3. *Chem. Phys. Lett.* **2014**, *598*, 75−80.
(65) Nziko, V. d. P. N.; Scheiner, S. Chalcogen Bonding between Tetravalent SF_4 and Amines. *J. Phys. Chem. A* **2014**, *118*, 10849−10856.

DOI: 10.1021/jp511828h
J. Phys. Chem. A 2015, 119, 535−541